

Exclusive photoproduction of charmonia in $\gamma p \rightarrow Vp$ and $pp \rightarrow pVp$ reactions within k_t -factorization approach

A. Cisek,^{1,*} W. Schäfer,^{2,†} and A. Szczurek^{2,1,‡}

¹*University of Rzeszów, PL-35-959 Rzeszów, Poland*

²*Institute of Nuclear Physics PAN, PL-31-342 Cracow, Poland*

(Dated: November 2, 2021)

Abstract

The amplitude for $\gamma p \rightarrow J/\psi p$ ($\gamma p \rightarrow \psi' p$) is calculated in a pQCD k_T -factorization approach. The total cross section for this process is calculated for different unintegrated gluon distributions and compared with the HERA data and the data extracted recently by the LHCb collaboration. The amplitude for $\gamma p \rightarrow J/\psi p$ ($\gamma p \rightarrow \psi' p$) is used to predict the cross section for exclusive photoproduction of J/ψ (ψ') meson in proton-proton collisions. Compared to earlier calculations we include both Dirac and Pauli electromagnetic form factors. The effect of Pauli form factor is quantified. Absorption effects are taken into account and their role is discussed in detail. Different differential distributions e.g. in J/ψ (ψ') rapidity and transverse momentum are presented and compared with existing experimental data. The UGDF with nonlinear effects built in better describe recent experimental data of the LHCb collaboration but no definite conclusion on onset of saturation can be drawn. We present our results also for the Tevatron. A good agreement with the CDF experimental data points at the midrapidity for both J/ψ and ψ' is achieved.

PACS numbers: 13.60.Le, 13.85.-t, 12.40.Nn, 14.40.Be

arXiv:1405.2253v1 [hep-ph] 9 May 2014

*Electronic address: acisek@univ.rzeszow.pl

†Electronic address: Wolfgang.Schafer@ifj.edu.pl

‡Electronic address: Antoni.Szczurek@ifj.edu.pl

I. INTRODUCTION

The exclusive production of J/ψ mesons in proton-proton and proton-antiproton scattering has recently attracted some interest [1–10].

In an early paper [5], it was shown that the exclusive production of J/ψ at the Tevatron is sensitive to the $\gamma p \rightarrow J/\psi p$ scattering in the similar region of energy as measured at HERA [11]. Given that fact the measured cross section for $\gamma p \rightarrow J/\psi p$ was parametrized and used in that calculation. Our predictions there could be successfully confronted with the Tevatron data [1] and good agreement was achieved [12]. The formalism proposed in [13] and used in [5] allows to calculate fully differential distributions for the three-body reaction in the broad range of four-dimensional phase space. The formalism proposed in [26] allows to test unintegrated gluon distributions (UGDFs) in the proton provided the quark-antiquark wave function of the meson is known. The experimental data for production of different vector mesons prefer Gaussian light-cone wave function [13–16].

Recently also the LHCb collaboration measured rapidity distributions of the J/ψ meson but rather in semi-exclusive reaction [2, 3]¹. Using some theoretical input from Ref.[5] the LHCb collaboration tried to extract the cross for the $\gamma p \rightarrow J/\psi p$ reaction at unprecedentedly high energies not available before at HERA, The procedure proposed uses some assumption which are only approximate and need further verification. Very recently the authors of Ref.[10] tried to use the pseudo-data to achieve information on integrated gluon distribution in very small x (longitudinal momentum fraction carried by the gluon) region, not available earlier at electron machines. The formalism applied in Ref.[10] uses a slightly simplified collinear formalism where the quark-antiquark wave function is replaced by a normalization constant [17]. In this formalism only rapidity distribution was discussed. In contrast to the collinear approach the k_t -factorization approach allows to study the complete kinematically reaction. In the present analysis we shall show how some UGDFs from the literature compare to the LHCb data [2, 3]. We leave the inclusion of the inelastic contribution as well as a possible fitting of UGDF for further studies. Compared to other calculations in the literature we include here not only the spin-conserving coupling but also the spin-flip one.

II. PHOTOPRODUCTION PROCESS $\gamma p \rightarrow J/\psi p$

The imaginary part of the forward amplitude sketched in Fig.1 can be written as [13, 14]:

$$\Im m \mathcal{M}_T(W, \Delta^2 = 0, Q^2 = 0) = W^2 \frac{c_v \sqrt{4\pi\alpha_{em}}}{4\pi^2} 2 \int_0^1 \frac{dz}{z(1-z)} \int_0^\infty \pi dk^2 \psi_V(z, k^2) \int_0^\infty \frac{\pi d\kappa^2}{\kappa^4} \alpha_S(q^2) \mathcal{F}(x_{\text{eff}}, \kappa^2) \left(A_0(z, k^2) W_0(k^2, \kappa^2) + A_1(z, k^2) W_1(k^2, \kappa^2) \right), \quad (2.1)$$

where, for the pure S -wave vector meson,

$$A_0(z, k^2) = m_c^2 + \frac{k^2 m_q}{M + 2m_c},$$

¹ The protons were not detected and only incomplete rapidity gap was checked.

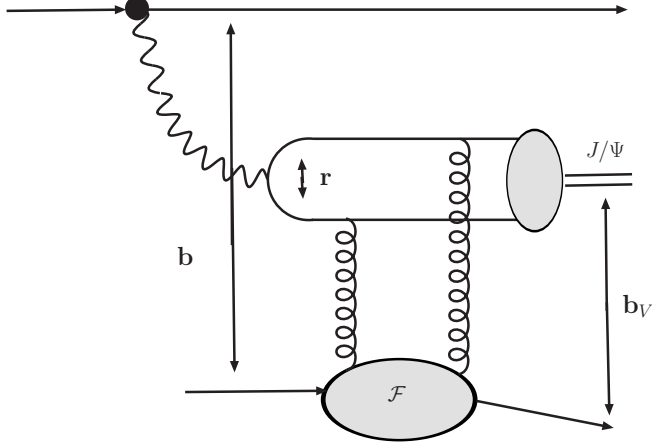


FIG. 1: Diagrams representing amplitude for the $\gamma p \rightarrow J/\psi p$ process.

$$A_1(z, k^2) = \left[z^2 + (1-z)^2 - (2z-1)^2 \frac{m_c}{M+2m_c} \right] \frac{k^2}{k^2 + m_c^2},$$

$$W_0(k^2, \kappa^2) = \frac{1}{k^2 + m_c^2} - \frac{1}{\sqrt{(k^2 - m_c^2 - \kappa^2)^2 + 4m_c^2 k^2}},$$

$$W_1(k^2, \kappa^2) = 1 - \frac{k^2 + m_c^2}{2k^2} \left(1 + \frac{k^2 - m_c^2 - \kappa^2}{\sqrt{(k^2 - m_c^2 - \kappa^2)^2 + 4m_c^2 k^2}} \right).$$

Here $\psi_V(z, k^2)$ is the meson light-cone wave function, $\mathcal{F}(x_{\text{eff}}, \kappa^2)$ is the unintegrated gluon distribution function. The invariant mass of the $c\bar{c}$ -system is given by

$$M = \sqrt{\frac{k^2 + m_c^2}{z(1-z)}} \quad (2.2)$$

We choose the scale of the QCD constant running coupling at $q^2 = \max\{\kappa^2, k^2 + m_c^2\}$. The full amplitude, at finite momentum transfer is given by:

$$\mathcal{M}(W, \Delta^2) = (i + \rho) \Im m \mathcal{M}(W, \Delta^2 = 0, Q^2 = 0) \exp(-B(W)\Delta^2/2), \quad (2.3)$$

where the real part of the amplitude is restored from analyticity,

$$\rho = \frac{\Re e \mathcal{M}}{\Im m \mathcal{M}} = \tan \left(\frac{\pi}{2} \frac{\partial \log (\Im m \mathcal{M} / W^2)}{\partial \log W^2} \right). \quad (2.4)$$

Above $B(W)$ is a slope parameter which in general depends on the photon-proton center-of-mass energy and is parametrized in the present analysis as:

$$B(W) = b_0 + 2\alpha'_{eff} \log \left(\frac{W^2}{W_0^2} \right), \quad (2.5)$$

with: $b_0 = 4.88$, $\alpha'_{eff} = 0.164 \text{ GeV}^{-2}$ and $W_0 = 90 \text{ GeV}$ [11].

Finally, the total cross section for diffractive J/ψ photoproduction on the nucleon can be calculated from:

$$\sigma(\gamma p \rightarrow J/\psi p) = \frac{1 + \rho^2}{16\pi B(W)} \left| \Im m \frac{\mathcal{M}(W, \Delta^2 = 0)}{W^2} \right|^2. \quad (2.6)$$

III. J/ψ AND ψ' WAVE FUNCTIONS

We include the Fermi-motion of quark and antiquark in the bound-state by means of the light-cone wave function of the vector meson.

While the light-cone wave function $\psi_V(z, k^2)$ is written as a function of the momentum fraction z of the quark and the relative transverse momentum \mathbf{k} of quarks in the bound state, in fact it depends only on the relative momentum \vec{p} of c and \bar{c} in the rest frame of the meson given by

$$\vec{p} = (\mathbf{p}, p_z) = (\mathbf{k}, (z - 1/2)M). \quad (3.1)$$

Following quite literally the approach of [13, 14] we use as an ansatz for the wave function dependence on \vec{p} :

$$\begin{aligned} \psi_{1S}(z, k^2) &= \psi_{1S}(\vec{p}^2) = c_1 \exp\left(-a_1^2 \vec{p}^2/2\right), \\ \psi_{2S}(z, k^2) &= \psi_{2S}(\vec{p}^2) = c_2 (\xi_{\text{node}} - a_2^2 \vec{p}^2) \exp\left(-a_2^2 \vec{p}^2/2\right). \end{aligned} \quad (3.2)$$

This functional dependence is obviously inspired by the harmonic-oscillator potential, notice however that following [13, 14] we keep a_1, a_2 which would be equal in the strict harmonic oscillator potential as free parameters. The parameters are fixed from the leptonic decay widths of J/ψ and ψ' , as well as from the orthonormality conditions of the $1S, 2S$ bound states. Recently a number of theoretical arguments for an effectively harmonic confinement potential on the light-front from various approaches have been given in [18].

Let us stress that an account of the wave function is important to make predictions for the production of excited charmonium states. While we use the momentum space formulation of diffractive vector meson production, the equivalent color-dipole formulation is more intuitive to understand the argument: it is the overlap of the light-cone wave functions of photon and vector meson which controls the effective dipole size distributions that enter the dipole cross section [19, 20]. Here especially the node in the wave function of the radial excitation has a subtle effect on the energy dependence [21].

Often an extreme nonrelativistic limit is adopted, in which heavy quarks are assumed to be at rest in the meson rest frame, and hence the momentum dependence of the wave function is neglected. Typically then also the transverse momentum of gluons is integrated out [17], and the diffractive amplitude becomes proportional to the integrated glue of the target. Strictly speaking in such an approximation one cannot predict the energy dependence of J/ψ vs. ψ' production, as to the accuracy of [17] it is illegitimate to differentiate between $2m_c$, the invariant mass of the $c\bar{c}$ pair, M , or the bound-state mass M_V , either of which could enter the hard scale. The wave function ‘‘node effect’’ [14, 20], which leads to a strong dependence of the $\psi'/J/\psi$ ratio on the bound-state wave function clearly cannot be accommodated in this way.

IV. EXCLUSIVE PHOTOPRODUCTION OF J/ψ IN pp AND $p\bar{p}$ COLLISIONS

The Born mechanism of the production of the J/ψ meson (similar mechanism for ψ') in proton-proton collisions is shown in Fig.2. There are two diagrams. In first diagram photon couples to the first proton while in the second diagram the photon couples to the second proton. The photon splits to a $c\bar{c}$ dipole which interacts with the other proton via exchange of gluonic ladder. The presence of two mechanisms leads to interference effects [5]. The interference effect leads to interesting azimuthal correlations between outgoing protons [5], never identified so far.

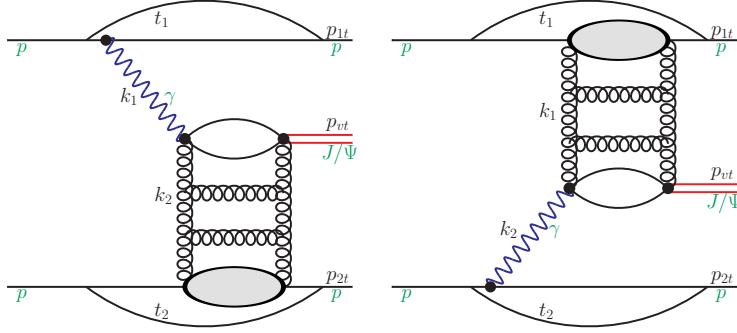


FIG. 2: Diagrams representing Born amplitudes considered for the $pp \rightarrow ppJ/\psi$ process.

The full Born amplitude for the $pp \rightarrow pVp$ process can be written as:

$$\begin{aligned} \mathcal{M}_{h_1 h_2 \rightarrow h_1 h_2 V}^{\lambda_1 \lambda_2 \rightarrow \lambda'_1 \lambda'_2 \lambda_V}(s, s_1, s_2, t_1, t_2) &= \mathcal{M}_{\gamma \mathbf{P}} + \mathcal{M}_{\mathbf{P} \gamma} \\ &= \langle p'_1, \lambda'_1 | J_\mu | p_1, \lambda_1 \rangle \epsilon_\mu^*(q_1, \lambda_V) \frac{\sqrt{4\pi\alpha_{em}}}{t_1} \mathcal{M}_{\gamma^* h_2 \rightarrow V h_2}^{\lambda_\gamma^* \lambda_2 \rightarrow \lambda_V \lambda_2}(s_2, t_2, Q_1^2) \\ &+ \langle p'_2, \lambda'_2 | J_\mu | p_2, \lambda_2 \rangle \epsilon_\mu^*(q_2, \lambda_V) \frac{\sqrt{4\pi\alpha_{em}}}{t_2} \mathcal{M}_{\gamma^* h_1 \rightarrow V h_1}^{\lambda_\gamma^* \lambda_1 \rightarrow \lambda_V \lambda_1}(s_1, t_1, Q_2^2). \end{aligned} \quad (4.1)$$

In terms of their transverse momenta $\mathbf{p}_{1,2}$ the relevant four-momentum transfers squared are $t_1 = -(\mathbf{p}_1^2 + z_1^2 m_p^2)/(1 - z_1)$ and $t_2 = -(\mathbf{p}_2^2 + z_2^2 m_p^2)/(1 - z_2)$ and $s_1 \approx (1 - z_2)s$ and $s_2 \approx (1 - z_1)s$ are the familiar Mandelstam variables.

Then, the amplitude of Eq. (4.1) for the emission of a photon of transverse polarization λ_V , and transverse momentum $\mathbf{q}_1 = -\mathbf{p}_1$ can be written as:

$$\langle p'_1, \lambda'_1 | J_\mu | p_1, \lambda_1 \rangle \epsilon_\mu^*(q_1, \lambda_V) = \frac{(\mathbf{e}^{(\lambda_V)} \cdot \mathbf{q}_1)}{\sqrt{1 - z_1}} \frac{2}{z_1} \chi_{\lambda'}^\dagger \left\{ F_1(Q_1^2) - \frac{i\kappa_p F_2(Q_1^2)}{2m_p} (\boldsymbol{\sigma}_1 \cdot [\mathbf{q}_1, \mathbf{n}]) \right\} \chi_\lambda. \quad (4.2)$$

Above χ_λ is its spinor, $\mathbf{e}^{(\lambda)} = -(\lambda \mathbf{e}_x + i \mathbf{e}_y)/\sqrt{2}$, $\mathbf{n} || \mathbf{e}_z$ denotes the collision axis, and $\boldsymbol{\sigma}_1/2$ is the spin operator for nucleon 1. F_1 and F_2 are respectively the Dirac and Pauli electromagnetic form factors, $\kappa_p = 1.79$.

Below the $2 \rightarrow 3$ bare amplitude (when absorption effects is ignored) is shown in the form of a 2-dimensional vector:

$$\mathbf{M}^{(0)}(\mathbf{p}_1, \mathbf{p}_2) = e_1 \frac{2}{z_1} \frac{\mathbf{p}_1}{t_1} \mathcal{F}_{\lambda'_1 \lambda_1}(\mathbf{p}_1, t_1) \mathcal{M}_{\gamma^* h_2 \rightarrow V h_2}(s_2, t_2, Q_1^2)$$

$$+e_2 \frac{2}{z_2} \frac{\mathbf{p}_2}{t_2} \mathcal{F}_{\lambda_2 \lambda_2}(\mathbf{p}_2, t_2) \mathcal{M}_{\gamma^* h_1 \rightarrow V h_1}(s_1, t_1, Q_2^2).$$

Because of the presence of the proton from factors only small Q_1^2 and Q_2^2 enter the amplitude for the hadronic process. This means that in practice, inside the photoproduction amplitude, one can put $Q_1^2 = Q_2^2 = 0$.

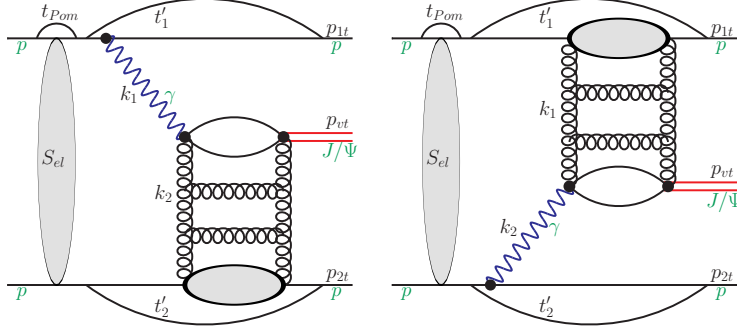


FIG. 3: Diagrams representing absorptive corrections considered for the $pp \rightarrow ppJ/\psi$ process.

The full amplitude for the $pp \rightarrow pJ/\psi p$ or $pptop\phi'p$ is calculated as:

$$\begin{aligned} \mathbf{M}(\mathbf{p}_1, \mathbf{p}_2) &= \int \frac{d^2\mathbf{k}}{(2\pi)^2} S_{el}(\mathbf{k}) \mathbf{M}^{(0)}(\mathbf{p}_1 - \mathbf{k}, \mathbf{p}_2 + \mathbf{k}) \\ &= \mathbf{M}^{(0)}(\mathbf{p}_1, \mathbf{p}_2) - \delta\mathbf{M}(\mathbf{p}_1, \mathbf{p}_2). \end{aligned} \quad (4.3)$$

The corresponding diagrams are shown in Fig.3. In the present calculations we include only elastic rescattering corrections. Then

$$S_{el}(\mathbf{k}) = (2\pi)^2 \delta^{(2)}(\mathbf{k}) - \frac{1}{2} T(\mathbf{k}), \quad T(\mathbf{k}) = \sigma_{tot}^{pp}(s) \exp\left(-\frac{1}{2} B_{el} \mathbf{k}^2\right). \quad (4.4)$$

In practical evaluations we take $B_{el} = 17 \text{ GeV}^{-2}$, $\sigma_{tot}^{pp} = 76 \text{ mb}$ [5, 22] for the Tevatron energy and $B_{el} = 19.89 \text{ GeV}^{-2}$, $\sigma_{tot}^{pp} = 98.6 \text{ mb}$ for the LHC energy [23].

The absorptive correction to the amplitude can be written as:

$$\delta\mathbf{M}(\mathbf{p}_1, \mathbf{p}_2) = \int \frac{d^2\mathbf{k}}{2(2\pi)^2} T(\mathbf{k}) \mathbf{M}^{(0)}(\mathbf{p}_1 - \mathbf{k}, \mathbf{p}_2 + \mathbf{k}).$$

Inelastic intermediate proton excitations can be taken into account effectively by multiplying elastic amplitudes by a constant bigger than 1.

V. RESULTS

A. J/ψ production

Before we go to the proton-proton processes let us first summarize our description of HERA data [11, 24, 25]. In Fig.4 we show results of calculations with the Ivanov-Nikolaev

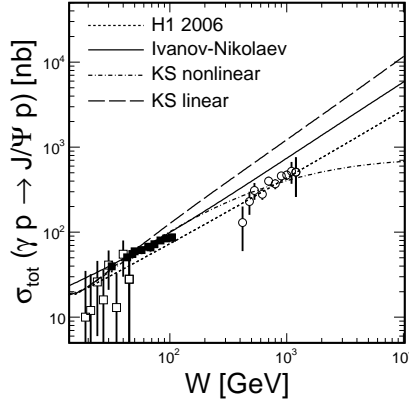


FIG. 4: Total cross section for the $\gamma p \rightarrow J/\psi p$ as a function of the subsystem energy together with the HERA data and pseudodata obtained by the LHCb collaboration. Three different UGDFs have been used: Ivanov-Nikolaev (solid), Kutak-Stasto linear (dashed) and Kutak-Stasto nonlinear (dash-dotted). The dotted line represents calculation with a simple power-like parametrization of the old HERA data [25]. The HERA data points [11] and the LHCb data points [2, 3] are shown for comparison.

[13, 26] and Kutak-Stasto [27] gluon unintegrated distributions. In the second case we consider both a BFKL version called linear and a version where gluon is obtained by solving Balitsky-Kovchegov evolution equation called nonlinear.

In Fig.5 we show rapidity distribution in the Born approximation for different UGDFs. The dashed line represents calculation when only vector (F_1) terms are included, while the solid line represents calculations with vector (F_1) and tensor (F_2) couplings of photon to the proton. The effect of taking into account tensor coupling is here of the order of 5 % only.

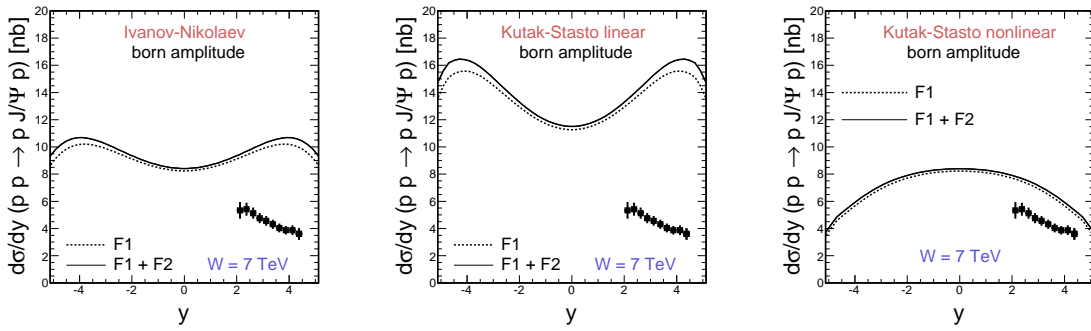


FIG. 5: J/ψ rapidity distribution calculated with the Born amplitudes for three different UGDFs from the literature for $\sqrt{s} = 7$ TeV. The dashed lines include contributions with Dirac F_1 electromagnetic form factor and the solid lines include in addition Pauli F_2 electromagnetic form factor. The new LHCb data points [3] are shown for comparison.

Similar distributions in J/ψ transverse momentum are shown in Fig.6. Large effect of the tensor coupling can be observed at large transverse momenta. At $p_t \sim \text{GeV}$ we get

an enhancement factor of the cross section of order of 10. Large transverse momenta are potentially interesting because of odderon exchange contribution (see e.g.[7]).

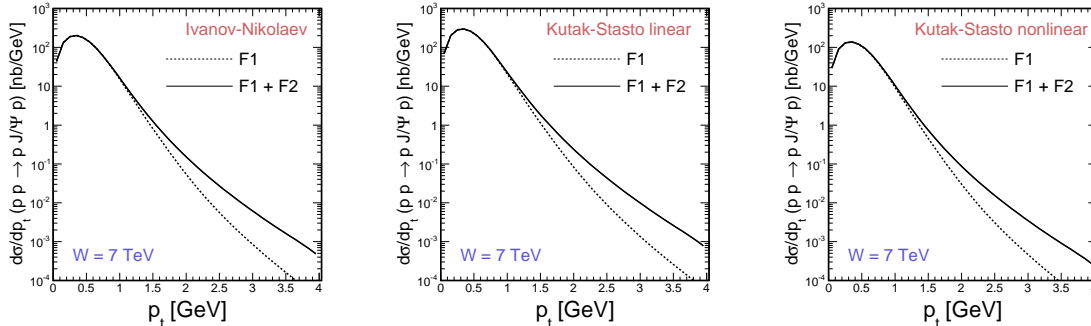


FIG. 6: J/ψ transverse momentum distribution calculated with the Born amplitudes for three different UGDFs from the literature for $\sqrt{s} = 7$ TeV. The dashed lines include contributions with Dirac F_1 electromagnetic form factor and the solid lines include in addition Pauli F_2 electromagnetic form factor.

The eikonal absorption damps rapidity distribution of J/ψ by about 30 % as is shown in Fig.7. The result with the Kutak-Stasto distribution which includes nonlinear effects is almost consistent with the newest LHCb data. Does it mean that we observe an onset of gluon saturation? We shall return to it in a while.

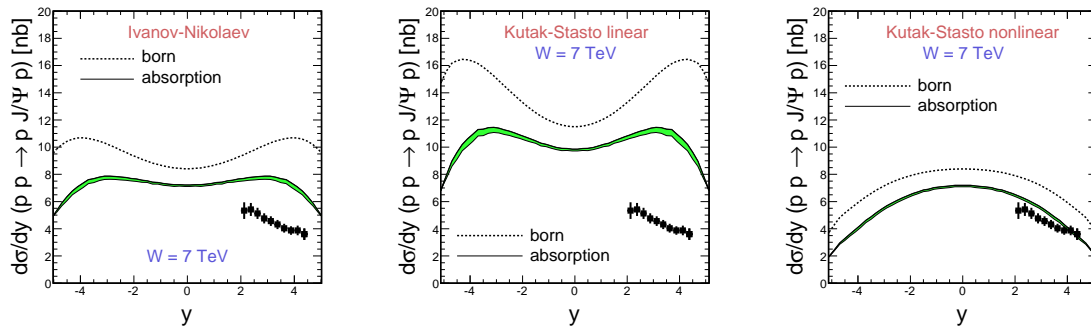


FIG. 7: J/ψ rapidity distribution calculated with inclusion of absorption effects (solid line), compared with the Born result (dashed line) for $\sqrt{s} = 7$ TeV. The new LHCb data points [3] are shown for comparison.

How the absorption modifies the J/ψ transverse momentum distribution is shown in Fig.8. The absorption leads to a strong damping at large J/ψ transverse momenta. This overcompensates the effect of inclusion of the tensor electromagnetic coupling quantified by the Pauli electromagnetic form factor. In Fig.8 we show both results with the standard absorption (elastic rescattering only) as well as with the absorption increased by a factor 1.4 to simulate inelastic (nucleon excitation) terms.

For completeness in Fig.9 we present rapidity (left panel) and transverse momentum (right panel) distributions obtained using H1 parametrization [25] of the elementary $\gamma p \rightarrow J/\psi p$

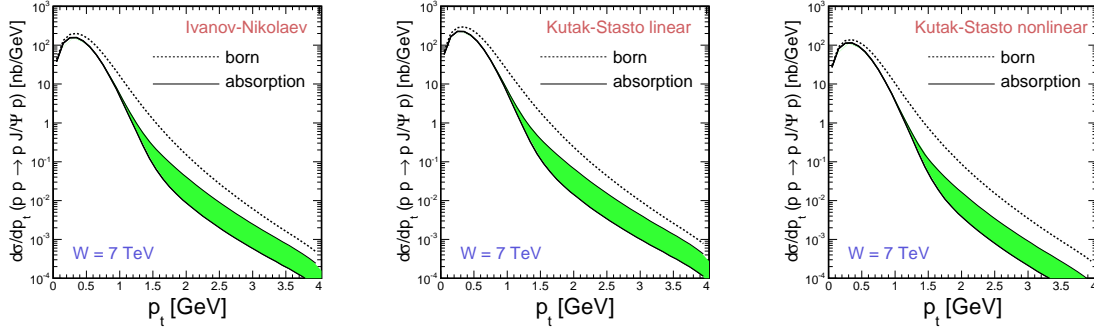


FIG. 8: J/ψ transverse momentum distribution calculated with with absorption effects (solid line) and in the Born approximation for $\sqrt{s} = 7$ TeV. The shaded (green online) band represents typical uncertainties in calculating absorption effects as described in the text.

cross section (see Fig.4). A good agreement with the LHCb data precludes drawing definite conclusion about onset of saturation.

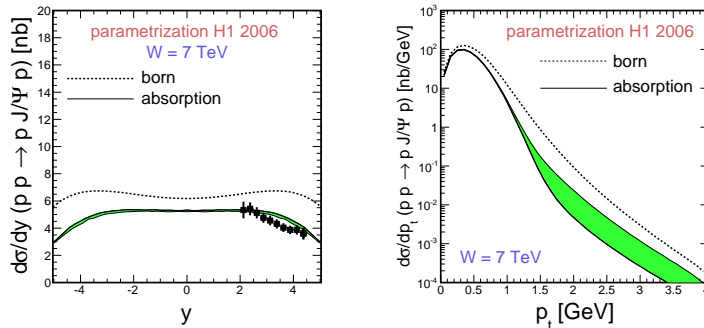


FIG. 9: J/ψ rapidity and transverse momentum distributions calculated with the H1 parametrization [5, 25] of the elementary $\gamma p \rightarrow J/\psi p$ cross section for $\sqrt{s} = 7$ TeV. The new LHCb data points [3] are shown for comparison.

B. ψ' production

Now we shall proceed to the production of the excited charmonium state ψ' . In Fig. 10 we present total cross section for the $\gamma p \rightarrow \psi' p$ as a function of collision energy for the different UGDFs considered here. Almost all the UGDFs provide good description of new HERA data [11]. The description seems better than in recent analysis in Ref.[29] where the collinear gluon distribution fitted to the production of J/ψ [10] was used. Part of the success is due to explicit use of light cone wave functions which are not explicit in the collinear approximation as discussed above.

Now we turn to hadronic collisions. In Fig.11 we present our predictions for rapidity distributions of ψ' again for different UGDFs. Results of our calculations are compared with recent LHCb data [3].

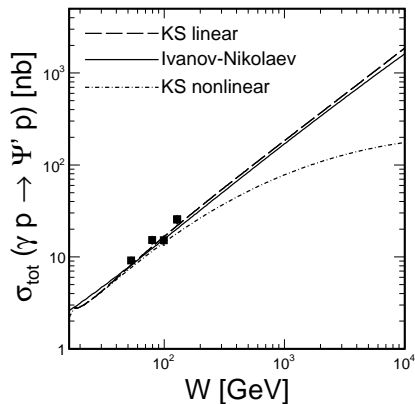


FIG. 10: Total cross section for the $\gamma p \rightarrow \psi' p$ as a function of the subsystem energy together with the HERA data and pseudodata obtained by the LHCb collaboration. Three different UGDFs have been used: Ivanov-Nikolaev (solid), Kutak-Stasto linear (dashed) and Kutak-Stasto nonlinear (dash-dotted). The experimental data are from Ref. [11].

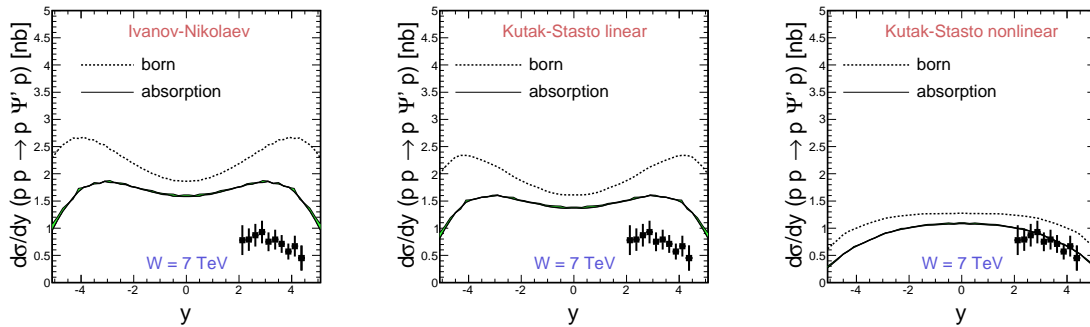


FIG. 11: Rapidity distribution of ψ' calculated with inclusion of absorption effects (solid line), compared with the result when absorption effects are ignored (dotted line) for $\sqrt{s} = 7$ TeV. The new LHCb data points [3] are shown for comparison.

The role of Pauli electromagnetic form factor is quantified in Fig.12. As for the ground state J/ψ the tensor coupling enhances the cross section at large meson transverse momenta.

The role of absorption effects is discussed in Fig.13. The Born results are shown for comparison. The absorption effects lead to strong damping of the cross section at large p_t 's. This is a region where odderon exchange may show up.

C. J/ψ and ψ' production at the Tevatron

In this section for completeness we present also results for the Tevatron. We repeat the same presentation as for the LHC. In Fig.14 we show distribution in rapidity of J/ψ . All UGDFs considered here describe the CDF data point if the absorption effects are included.

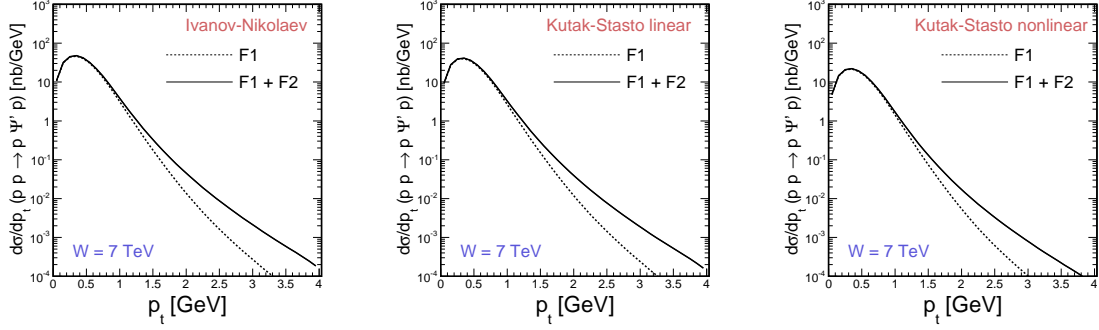


FIG. 12: ψ' transverse momentum distribution calculated in the Born approximation with and without including Pauli electromagnetic form factor for $\sqrt{s} = 7$ TeV.

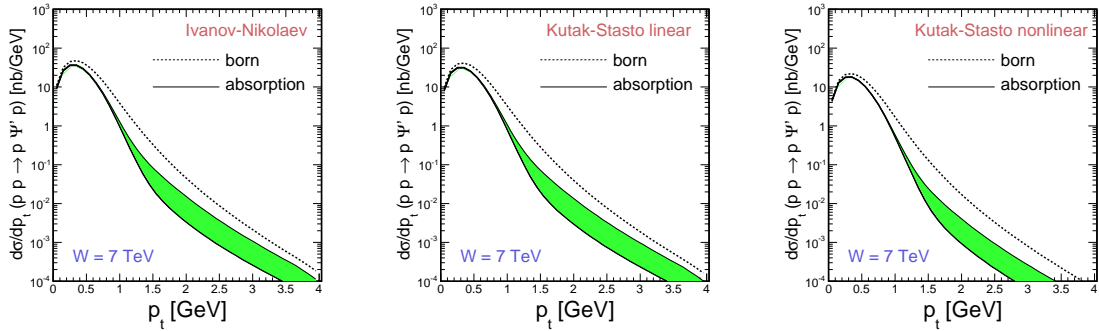


FIG. 13: ψ' transverse momentum distribution calculated with absorption effects (solid line) and in the Born approximation (dashed line) for $\sqrt{s} = 7$ TeV.

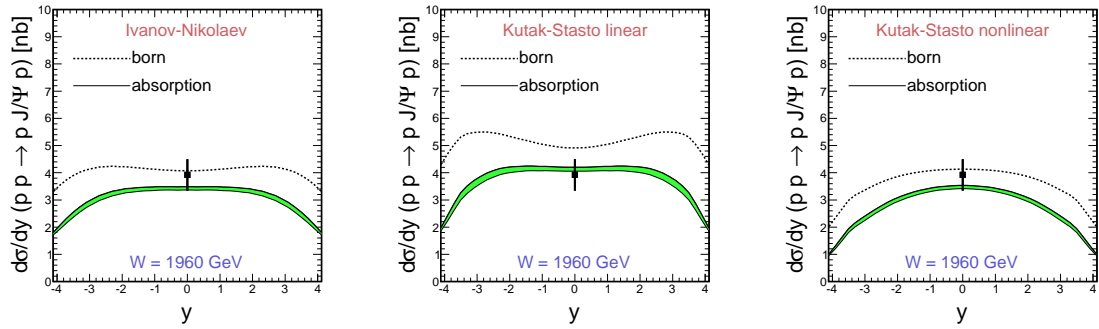


FIG. 14: J/ψ rapidity distribution calculated with inclusion of absorption effects (solid line), compared with the Born result (dashed line) for $\sqrt{s} = 1.96$ TeV. The CDF data point [1] is shown for comparison.

In the next figure (Fig.15) we demonstrate the role of the Pauli form factor on the J/ψ transverse momentum distribution. The distributions for the Tevatron (larger x values of

the gluon distribution) drop much quicker than those for the LHC (lower x values of the gluon distribution). The role of absorption is presented in Fig.16.

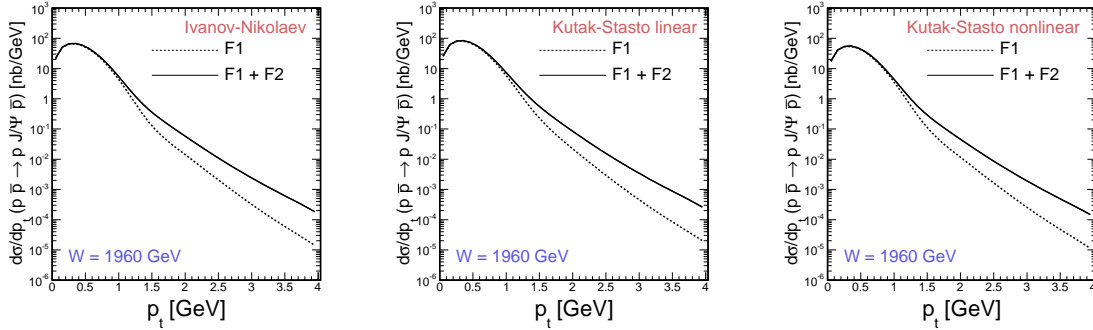


FIG. 15: J/ψ transverse momentum distribution calculated with the Born amplitudes for three different UGDFs from the literature for $\sqrt{s} = 1.96$ TeV. The dashed lines include contributions with Dirac F_1 electromagnetic form factor and the solid lines include in addition Pauli F_2 electromagnetic form factor.

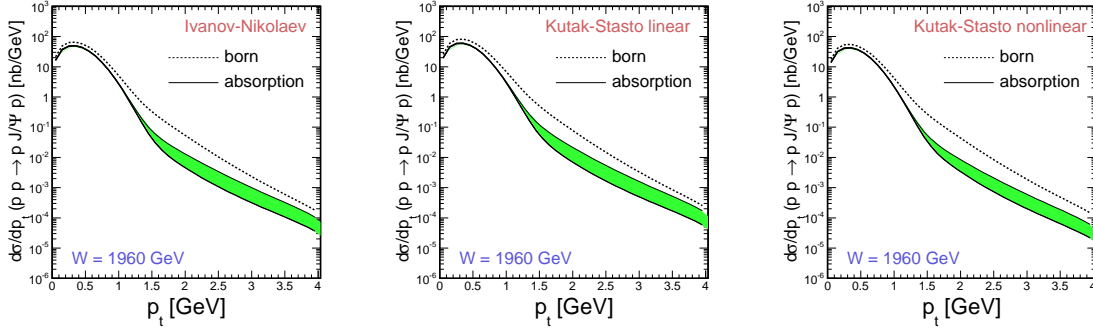


FIG. 16: J/ψ transverse momentum distribution calculated with absorption effects (solid line) and in the Born approximation (dashed line).

The same distributions but for exclusive ψ' production are shown in Figs.17,18, 19. The shape of the distributions is very similar as for the J/ψ meson. The corresponding cross section is, however, much smaller. Again we nicely describe the Tevatron experimental point at midrapidity.

Summarizing the situation at the Tevatron, we nicely describe experimental data points at midrapidity both for exclusive J/ψ and ψ' production which gives further credibility to our approach.

VI. CONCLUSIONS

In the present paper we have reconsidered exclusive production of J/ψ meson in the $\gamma p \rightarrow J/\psi p$ and $pp \rightarrow ppJ/\psi$ reactions within the k_t -factorization formalism. First the total

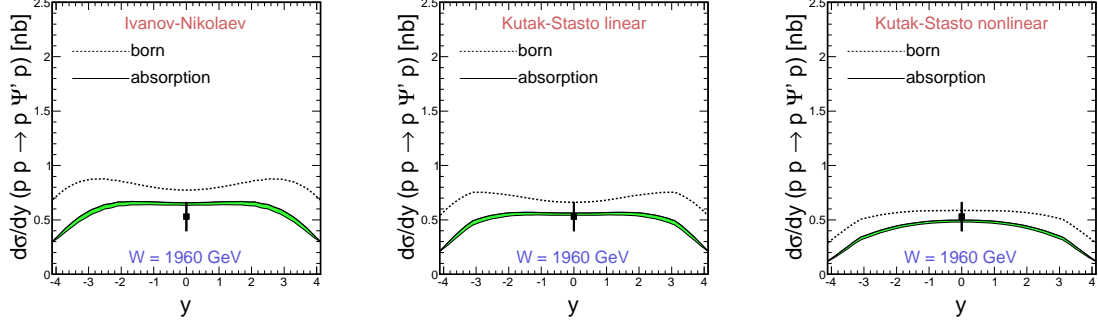


FIG. 17: Rapidity distribution of ψ' calculated with inclusion of absorption effects (solid line), compared with the result when absorption effects are ignored (dotted line) for $\sqrt{s} = 1.96$ TeV. The CDF data point [1] is shown for comparison.

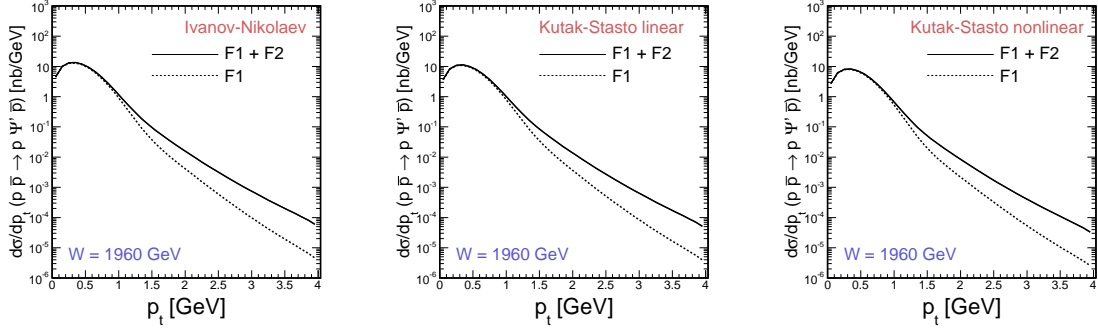


FIG. 18: ψ' transverse momentum distribution calculated in the Born approximation with and without including Pauli electromagnetic form factor for $\sqrt{s} = 1.96$ TeV.

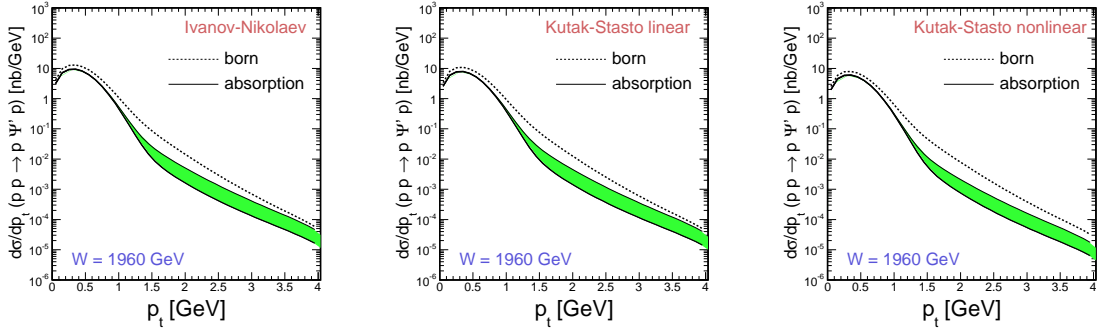


FIG. 19: ψ' transverse momentum distribution calculated with absorption effects (solid line) and in the Born approximation (dashed line) for $\sqrt{s} = 1.96$ TeV.

cross section for the $\gamma p \rightarrow J/\psi p$ reaction was calculated as a function of the subsystem energy and confronted with the HERA data for three different unintegrated distributions

from the literature.

In comparison to our earlier calculations in the past [5] in the present paper we have taken into account both the coupling of photons via spin-conserving vector coupling with F_1 Dirac electromagnetic form factor as well as spin-flipping tensor coupling with F_2 Pauli electromagnetic form factor for the $pp \rightarrow pJ/\psi p$ and $pp \rightarrow p\psi' p$ reactions. In distinction to the collinear approach, the theoretical approach used here allows to calculate many differential distributions for the three-body reaction $pp \rightarrow ppJ/\psi$. We have calculated not only J/ψ rapidity distribution but also distributions in J/ψ transverse momentum and distributions in four-momenta squared t_1 or t_2 . The role of the tensor coupling with the strength quantified by Pauli electromagnetic form factor F_2 . The tensor coupling is important for large $|t_1|$ or $|t_2|$ and as a consequence also for large transverse momenta of J/ψ . We have also carefully discussed the role of soft rescatterings which leads to a shape deformation of all distributions in contrast to commonly used uniform factor known as gap survival factor. The uncertainties related to the absorption effects have been discussed. We have shown that inclusions of inelastic rescatterings leads to further significant damping of the cross section at the large transverse momenta of J/ψ and ψ' .

Our calculations have been performed for different unintegrated gluon distributions used previously in the literature. The best agreement with the recent LHCb collaboration data has been achieved with UGDF which incorporates nonlinear effects in its evolution. This suggests an onset of saturation effects, especially for large J/ψ rapidities. Since a simple parametrization of the experimental cross section for $\gamma p \rightarrow J/\psi$ reaction also leads to a relatively good description of the LHCb data no definite conclusion on the onset of saturation can be drawn.

We have presented our results also for the Tevatron. A good agreement with the CDF experimental data point at the midrapidity for both J/ψ and ψ' has been achieved.

In the future we plan to find a phenomenological UGDF which simultaneously describes the F_2 deep-inelastic structure function data and the LHCb collaboration data for semi-exclusive production of J/ψ . Then the photonic-inelastic contributions (the exchanged photon leaves the remaining system in an excited state) must be taken into account in the analysis in a similar fashion as recently done for $\mu^+\mu^-$ semi-exclusive production [30]. This clearly goes beyond the scope of the present paper.

Acknowledgments

We would like to thank to Ronan McNulty for a discussion of the LHCb data. This work was partially supported by the Polish MNiSW grant DEC-2011/01/B/ST2/04535 as well as by the Centre for Innovation and Transfer of Natural Sciences and Engineering Knowledge in Rzeszów.

-
- [1] T. Aaltonen *et al.* [CDF Collaboration], Phys. Rev. Lett. **102**, 242001 (2009).
 - [2] R. Aaij *et al.* [LHCb Collaboration], J. Phys. G **40**, 045001 (2013).
 - [3] R. Aaij *et al.* [LHCb Collaboration], J. Phys. G **41**, 055002 (2014).
 - [4] S. R. Klein and J. Nystrand, Phys. Rev. Lett. **92**, 142003 (2004).
 - [5] W. Schäfer and A. Szczurek, Phys. Rev. **D76** (2007) 09014.
 - [6] L. Motyka and G. Watt, Phys. Rev. **D78** (2008) 014023, arXiv:0805.2113.

- [7] A. Bzdak, L. Motyka, L. Szymanowski and J.-R. Cudell, Phys. Rev. **D75** (2007) 094023.
- [8] V. P. Goncalves and M. V. T. Machado, Phys. Rev. C **84**, 011902 (2011).
- [9] M. B. Gay Ducati, M. T. Griep and M. V. T. Machado, Phys. Rev. D **88**, 017504 (2013).
- [10] S. P. Jones, A. D. Martin, M. G. Ryskin and T. Teubner, JHEP **1311**, 085 (2013).
- [11] C. Alexa *et al.* [H1 Collaboration], Eur. Phys. J. C **73** (2013) 2466.
- [12] Anna Cisek, PhD Thesis in The Henryk Niewodniczański Institute of Nuclear Physics Polish Academy of Sciences, Kraków, Poland, 2012.
- [13] I. P. Ivanov, N. N. Nikolaev and A. A. Savin, Phys. Part. Nucl. **37** (2006) 1.
- [14] I. P. Ivanov, “Diffractive production of vector mesons in deep inelastic scattering within $k(t)$ factorization approach,” hep-ph/0303053; PhD Thesis, Bonn University.
- [15] A. Rybarska, W. Schäfer and A. Szczurek, Phys. Lett. **B668** (2008) 126.
- [16] A. Cisek, W. Schäfer and A. Szczurek, Phys. Lett. **B690** (2010) 168.
- [17] M.G. Ryskin, Z. Phys. **C57** (1993) 89.
- [18] A. P. Trawiński, S. D. Glazek, S. J. Brodsky, G. F. de Teramond and H. G. Dosch, arXiv:1403.5651 [hep-ph].
- [19] N. N. Nikolaev, Comments Nucl. Part. Phys. **21**, 41 (1992).
- [20] B. Z. Kopeliovich, J. Nemchick, N. N. Nikolaev and B. G. Zakharov, Phys. Lett. B **309**, 179 (1993).
- [21] J. Nemchik, N. N. Nikolaev, E. Predazzi and B. G. Zakharov, Z. Phys. C **75**, 71 (1997).
- [22] CDF collaboration, F. Abe, Phys. Rev. **D50** (1994) 5518.
- [23] TOTEM collaboration, G. Antchev et al., Eur. Phys. Lett. **101** (2013) 21002.
- [24] H1 collaboration, C. Adloff et al., Phys. Lett. **B541** (2002) 251, .
- [25] H1 collaboration, A. Aktas et al., Eur. Phys. J. **C46** (2006) 585, .
- [26] I. P. Ivanov and N.N. Nikolaev, Phys. Rev. **D65** (2002) 054004,
- [27] K. Kutak and A. M. Staśto, Eur. Phys. J. **C49** (2005) 343.
- [28] A. Cisek, P. Lebiedowicz, W. Schäfer and A. Szczurek, Phys. Rev. **D83** (2011) 114004.
- [29] S. P. Jones, A. D. Martin, M. G. Ryskin and T. Teubner, J. Phys. G **41**, 055009 (2014).
- [30] L. Forthomme, J. Hollar, K. Piotrkowski, G. de Silveira, W. Schäfer and A. Szczurek, a paper in preparation.

